

Electronic transport properties of molecular bipyridine junctions: Effects of isomer and contact structures

Zong-Liang Li, Bin Zou, and Chuan-Kui Wang*

College of Physics and Electronics, Shandong Normal University, Jinan 250014, China

Yi Luo

Theoretical Chemistry, Royal Institute of Technology, AlbaNova, S-10691 Stockholm, Sweden

(Received 19 July 2005; revised manuscript received 9 November 2005; published 24 February 2006)

The effects of contact structures and isomers on the current-voltage characteristics of molecular bipyridine junctions have been investigated by means of a generalized quantum chemical approach based on the elastic scattering Green's function method. For the four isomers 4,4'-bipyridine, 2,2'-bipyridine, 2,4'-bipyridine, and 2,6'-bipyridine under investigation, the 2,4'-bipyridine junction is found to be the poorest conductor owing to its nonsymmetrical arrangement. Numerical simulations of the 4,4'-bipyridine junction show that the contact structures between molecule and metallic electrodes have a noticeable effect on the electron transport characteristics of molecular junctions. The shortening of the distance between two metallic electrodes results in a stronger coupling and lower potential barrier between them, leading to larger conductance. The external electric fields cause the charge redistribution within molecule and lead to the presence of resistivity dipoles at the molecule-metal interface, and the bias voltages are mainly dropped there. The nonlinear charge transport effect on the current and conductance of 4,4'-bipyridine molecular junctions at the lower-bias region is presented. The experimental measurement has been reproduced by the theoretical calculations for a well-defined structure.

DOI: [10.1103/PhysRevB.73.075326](https://doi.org/10.1103/PhysRevB.73.075326)

PACS number(s): 73.63.-b, 85.65.+h, 73.63.Rt, 31.15.Ar

I. INTRODUCTION

With the continuous miniaturization of electronic devices, molecular electronic devices are considered as appropriate candidates for nanometer electronics. Currently, many exciting results have been obtained in areas of single-molecular electronics.¹⁻⁸ After the pioneering work in measuring the electronic properties of a single-molecular wire using benzene-1,4-dithiolate at room temperature with a mechanically controllable break junction by Reed *et al.*,¹ a few groups have pursued actively to investigate the electric characteristics of different molecules and found that a single-molecular device has many interesting features such as negative differential resistance^{3,4} and field-effect modulation. Based on these properties, some functional molecular devices—for instance, molecular transistors, molecular switches,⁶ and molecular rectifiers—have been designed. Most recently, Xu and Tao⁸ have determined the conductance of single molecular devices containing a 4,4'-bipyridine and a N-alkanedithiol connected to gold electrodes by repeatedly forming thousands of gold-molecule-gold junctions and elucidated that the chemical bonding between molecule and metal is very important for electronic transportation. They also conclude that the conductance of N-alkanedithiols decreases exponentially with the length of the molecule which has been verified by the other experimental and theoretical studies.⁹

Most theoretical studies of electron transport in molecular electronic devices are based on the solid-state physics approach.¹⁰⁻¹³ The agreement between theory and experiment is, however, generally poor. This has been largely attributed to a lack of information about molecule-metal con-

tacts in experiments. In theoretical simulations, the electrodes were often modeled by ideal metal surfaces. However, the experiments were carried out at ambient conditions with mechanical break junctions. It is thus desirable to study the effect of the local contact structures on the conductance properties of the molecular junctions. Our quantum chemical approach¹⁴⁻¹⁷ is particularly feasible for such a study since our model allows us to use any desirable contact geometry.

In our previous work,¹⁴⁻¹⁷ we adopted an approximation that the interaction between the molecule and metal occurs only through the end sites of the molecule. Recently, we have generalized this approach to include interactions among all sites in the device and it has been implemented with the QCME program.¹⁸ With it, the calculated current-voltage characteristics of alkanemonothiol and alkanedithiol molecular junctions are found to be in good agreement with the experiments.⁹ In this report, we investigate the electron transport properties of organic molecular bipyridine devices with gold electrodes. Four isomers 4,4'-bipyridine, 2,2'-bipyridine, 2,6'-bipyridine, and 2,4'-bipyridine have been studied. For 4,4'-bipyridine devices, three different contact geometries are considered: (i) a surface with seven gold atoms (cont1), (ii) a linear chain of three gold atoms (cont2), and (iii) a pyramid structure with seven gold atoms (cont3). It is noted that the 4,4'-bipyridine molecule is physically connected with the gold electrodes. The bonding distance between the molecule and metal electrodes is thus difficult to determine from the experimental measurements. We have thus examined the bond length dependence of the conductance of the devices with different contact structures in detail. The potential distributions of different configurations have also been presented. We have found that good

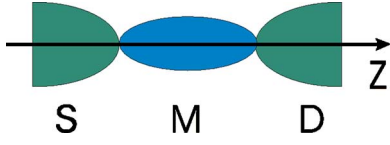


FIG. 1. (Color online) Scheme of the molecular junction.

agreement between theory and experiment can be achieved for a particular stable configuration.

II. THEORETICAL METHOD AND COMPUTATIONAL DETAILS

The molecular junction is schematically shown in Fig. 1, where M represents a molecule and S and D are electron reservoirs. Here the molecule that we will investigate is 4,4'-bipyridine. For a three-dimensional electrode, when an external bias V is applied, the net current density of the device from the source to the drain can be written as¹⁷

$$j = \frac{4emk_B T}{\hbar^3} \int \left\{ \ln \left[1 + \exp \left(\frac{E_f - E_z + eV}{k_B T} \right) \right] - \ln \left[1 + \exp \left(\frac{E_f - E_z}{k_B T} \right) \right] \right\} |T(E_z, V)|^2 n_{1D}^S(E_z) n_{1D}^D(E_z) dE_z. \quad (1)$$

Then the total current from S to D is

$$I = Aj = \pi r_{3s}^2 j = \left(\frac{9\pi}{4} \right)^{1/3} \frac{9ek_B T}{2\hbar E_f^2} \times \int \left\{ \ln \left[1 + \exp \left(\frac{E_f - E_z + eV}{k_B T} \right) \right] - \ln \left[1 + \exp \left(\frac{E_f - E_z}{k_B T} \right) \right] \right\} |T(E_z, V)|^2 \frac{dE_z}{E_z}. \quad (2)$$

Therefore the differential conductance can be written as

$$G = \frac{\partial I}{\partial V}. \quad (3)$$

The choice of the Fermi level is a major problem for the modeling of single-molecular transport. In our calculations, the middle of highest occupied and lowest unoccupied molecular orbitals (HOMO and LUMO) of the metal-molecule cluster is chosen as the Fermi level, and the nonequilibrium transport is considered by simply lining up the Fermi energy of the extended molecule and bulk metals.

In Eq. (1), the transition probability $|T(E, V)|^2$ can be determined by¹⁴

$$|T(E, V)|^2 = \left(\sum_{kk'} \sum_n Y_{Dk'}(V) Y_{kS}(V) \frac{\langle k'|n\rangle \langle n|k\rangle}{(E - E_n(V))^2 + \Gamma_{n,kk'}^2} \times [E - E_n(V)] \right)^2 + \left(\sum_{kk'} \sum_n Y_{Dk'}(V) Y_{kS}(V) \frac{\langle k'|n\rangle \langle n|k\rangle}{(E - E_n(V))^2 + \Gamma_{n,kk'}^2} \Gamma_{n,kk'} \right)^2, \quad (4)$$

where $k(k')$ runs over all atomic sites, which are denoted as $1, 2, \dots, J$, sites 1 and J are two end sites of molecule that connect with two electron reservoirs, and the orbital $|n\rangle$ is the eigenstate of the Hamiltonian of the composite cluster-molecule-cluster system, $H_f|n\rangle = E_n|n\rangle$. The product of two overlap matrix elements $\langle k'|n\rangle \langle n|k\rangle$ describes the delocalization of orbital $|n\rangle$. E is the energy at which the scattering process is observed. $Y_{kS}(V)$ and $Y_{Dk'}(V)$ represent the couplings between the k atom of the molecule and the gold clusters (noted by S and D) in the site representation,

$$\begin{aligned} Y_{kS}(V) &= \langle k|U|S\rangle = \sum_{n,\alpha,i} C_{n\alpha}^k \langle k_\alpha|U|S_i\rangle C_{ni}^S \\ &= \sum_{n,\alpha,i} C_{n\alpha}^k \langle k_\alpha|H|S_i\rangle C_{ni}^S, \\ Y_{Dk'}(V) &= \langle D|U|k'\rangle = \sum_{n,\beta,j} C_{nj}^D \langle D_j|U|k'_\beta\rangle C_{n\beta}^{k'} \\ &= \sum_{n,\beta,j} C_{nj}^D \langle D_j|H|k'_\beta\rangle C_{n\beta}^{k'}, \end{aligned} \quad (5)$$

where $C_{n\alpha}^k$ ($C_{n\beta}^{k'}$) is the expansion coefficient of the orbital $|n\rangle$ on the atomic orbital $|\alpha\rangle$ ($|\beta\rangle$) of the atom k (k') of the molecule and C_{ni}^S (C_{nj}^D) is on the atomic orbital $|i\rangle$ ($|j\rangle$) of the gold atom cluster S (D).

The energy broadening $\Gamma_{n,kk'}$ is determined by calculating the imaginary part of the self-energy,^{19–22}

$$\begin{aligned} \Gamma_{n,kk'}(E) &= \Delta_{kS} + \Delta_{Dk'} = \pi Y_{kS}^2 |\langle n|k\rangle|^2 n^S(E) \\ &\quad + \pi Y_{Dk'}^2 |\langle k'|n\rangle|^2 n^D(E), \end{aligned} \quad (6)$$

where $n^{S(D)}$ is the density of states of the source and drain.

In our previous work,^{14–17} only the interaction between the end-site atoms of molecule and metal electrodes was considered and calculated according to the frontier molecular orbital concept. In the present formalism, couplings between the atomic sites of molecule and the electrodes are calculated analytically. All the occupied molecular orbitals $\{|n\rangle\}$ are included in the determination of Y_{kS} and $Y_{Dk'}$.

The geometry optimization and electronic structure calculations are performed at the hybrid density-functional theory (DFT) B3LYP level with Lan12DZ basis set in the GAUSSIAN03 package,²³ where the effective core potential (ECP) is used for the gold atoms. The electron transport properties are obtained from the QCME program.¹⁸

III. NUMERICAL RESULTS AND DISCUSSIONS

A. Linear transport response

In this section, we do not consider the influence caused by applied electronic fields on transport properties of molecular junctions. The exact geometry of the junction is not known from the experiment. We first assume that the contact resembles the gold (111) surface. In this case, there are three possible positions for the molecule to sit: namely, on the top of one gold atom, on the bridge of two gold atoms, or on the hollow position of three gold atoms. We have chosen a clus-

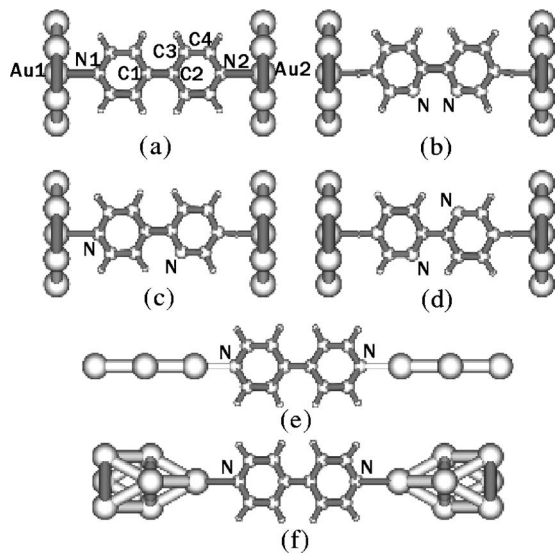


FIG. 2. Structures of isomer junctions. The surface contact with seven gold atoms at each side for (a) 4,4'-bipyridine, (b) 2,2'-bipyridine, (c) 2,4'-bipyridine, and (d) 2,6'-bipyridine. The chain contact with three gold atoms at each side (e) and pyramid contact with seven gold atoms at each side (f) for 4,4'-bipyridine.

ter of seven gold atoms with equilateral hexagon to model the gold surface (cont1). Two identical clusters are then connected by the molecule, where the main molecular axis is perpendicular to the equilateral hexagon (see Fig. 2). The geometric optimization of the 4,4'-bipyridine junction shows that it is energetically favorable for the nitrogen to sit on the top of the center gold atom and the equilibrium distance between two gold clusters is 1.26 nm. We have fixed this distance for the other three molecules to examine the isomer dependence of the electron transport properties.

The upper parts of Fig. 3 show the current and conductance curves for four isomers. For 4,4'-bipyridine and 2,4'-bipyridine molecular junctions, there are current gaps around 1.7 V and 2.3 V, respectively, while for 2,2'-bipyridine and 2,6'-bipyridine molecular junctions, their current gaps become narrower. Moreover, the current is gradually increased from 1.0 V for 2,2'-bipyridine and 0.4 V for 2,6'-bipyridine. The narrower current gap is largely due to the short distances between the molecule and gold clusters. At 3.5 V bias, the currents of 4,4'-bipyridine, 2,2'-bipyridine, and 2,6'-bipyridine junctions are all around $0.6 \mu\text{A}$, but only $0.3 \mu\text{A}$ for the 2,4'-bipyridine junction. From Fig. 3, one can observe that the conductance curves show plateau features. In the lower-bias regime, the conductance of all four molecular systems is close to zero. The first onset of the conductance curve for four molecular junctions appears at different biases, 1.7 V for 4,4'-bipyridine, 3 V for both 2,2'-bipyridine and 2,6'-bipyridine, and 2.3 V for 2,4'-bipyridine. Furthermore, in the bias regime under investigation, there exist three onsets for 4,4'-bipyridine, two for 2,4'-bipyridine, and only one for 2,2'-bipyridine and 2,6'-bipyridine molecular junctions. The conductance curves can be well understood by inspecting the corresponding transmission spectra given in the lower parts of Fig. 3. The onsets of conductance correspond to different electron

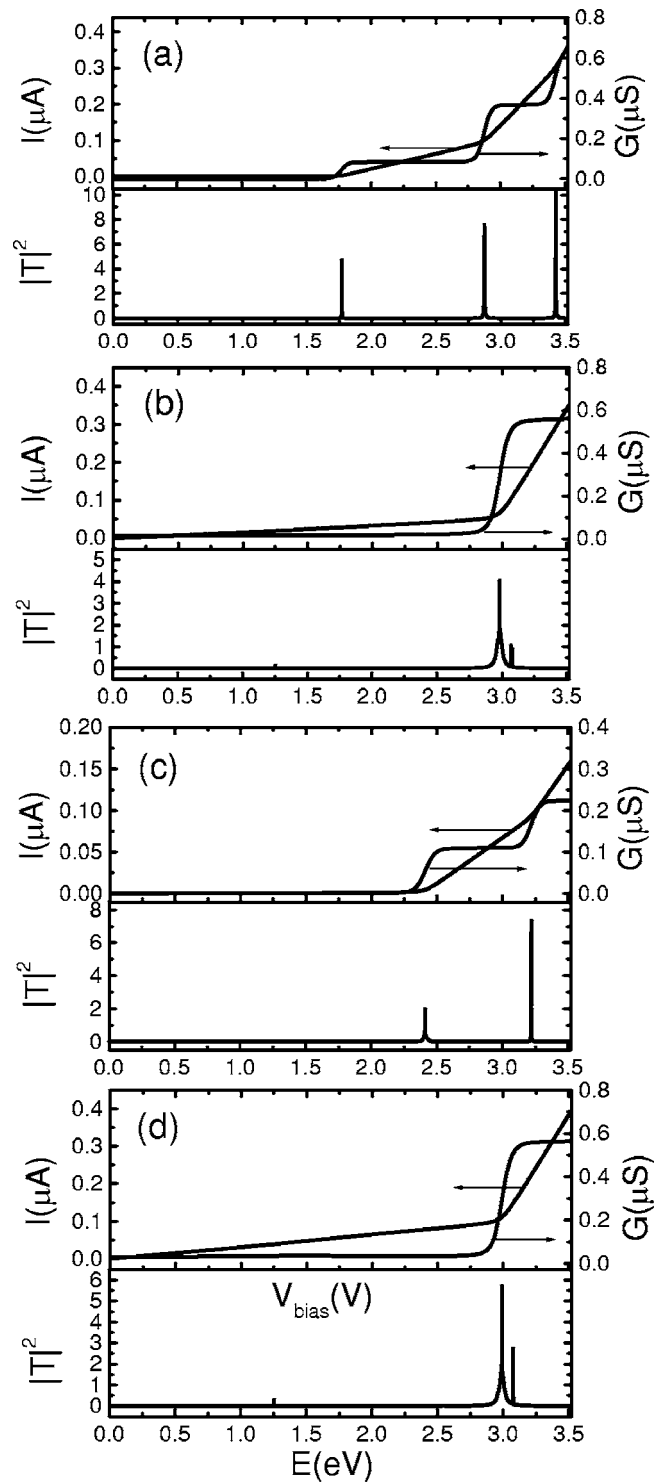


FIG. 3. Current and conductance of isomer junctions shown in Figs. 2(a)–2(d) together with transmission.

transport channels—i.e., the conductive molecular orbitals.^{24,25}

We now turn our attention to the effect of contact geometry and molecule-electrode distance on the electron transport properties. 4,4'-bipyridine is used as the model system. The molecular geometry is optimized for all cases. The optimized structures with cont1 for different distances of the

TABLE I. The optimized structure of 4,4'-bipyridine junction as shown in Fig. 2(a) with different distances of the two gold clusters.

d (Au1-Au2)	Bond length (Å)						
	N1-N2	Au1-N1	N2-Au2	C1-C2	C2-C3	C3-C4	C4-N2
10.6	6.58	2.01	2.01	1.41	1.39	1.36	1.33
10.8	6.69	2.05	2.05	1.42	1.40	1.36	1.33
11.0	6.79	2.11	2.11	1.43	1.40	1.37	1.34
11.2	6.88	2.16	2.16	1.44	1.40	1.38	1.34
11.6	7.11	2.25	2.25	1.48	1.41	1.40	1.35

two gold clusters are listed in Table I. One can see that, when the junction is stretched from 1.06 nm to 1.16 nm, the molecule is lengthened from 0.658 nm to 0.711 nm, an increase of 8% while the N1-Au1 bond is increased by 12%. Furthermore, the intramolecular changes are very small.

The calculated current and conductance curves for 4,4'-bipyridine with cont1 are shown in Fig. 4 as a function of the distance between two gold clusters. It is seen from Fig. 4(a) that currents are nonlinearly increased with the increase of the bias. Furthermore, currents are also strongly dependent on the distance between the electrodes. In general, longer distance results in smaller current. For instance, at an external bias of 1.0 V, the current for the device with distance of 1.06 nm is 4 μ A, which is about 20 times larger than that for the device with distance of 1.12 nm. Figure 4(b) shows the corresponding conductance of the molecular junctions. One can see that there exists a conductance plateau around zero bias. When the distance between the two gold clusters decreases, the value of the plateau increases and the plateau becomes narrower. At $d=1.06$ nm, the conductance reaches 9 μ S at a bias of 1.5 V, while it is just 2 μ S for $d=1.12$ nm. It can be concluded that the change of the distance between two electrodes can result in a significant change of the molecule-metal interaction and therefore the electron transport properties of the device.

We then choose another contact structure with three gold atoms in a straight line (cont2). The current and conductance

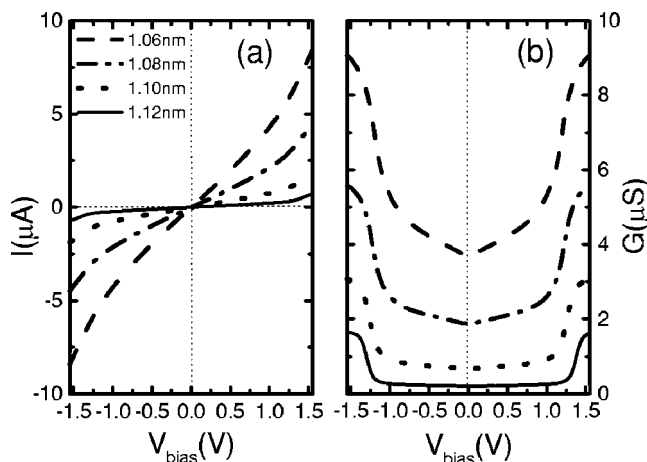


FIG. 4. Current (a) and conductance (b) curves of the molecular junction shown in Fig. 2(a). Distances of the two gold clusters are taken as $d=1.06$ nm (dashed line), 1.08 nm (dash-dotted line), 1.10 nm (dotted line), and 1.12 nm (solid line).

curves of the molecular junction are shown in Fig. 5 for different distances. They show similar features compared to those in Fig. 4. However, the values of the conductance plateau around zero bias are pushed down and the plateau becomes narrower compared to counterparts in Fig. 4(b). Therefore, the onset of the conductance starts at a lower bias as shown in Fig. 5(b). We have found that the calculated current-voltage characteristics of the device with two gold chain electrodes separated by a distance of 1.08 nm in Fig. 5(c) are in good agreement with the experimental result [see Fig. 2(E) in Ref. 8].

In order to further display the effect of contact structure on the electronic transport properties of molecular junction, we consider a pyramid structure with seven gold atoms (cont3) [see Fig. 2(f)]. Figure 6 shows the current and conductance curves for different distances between the two gold

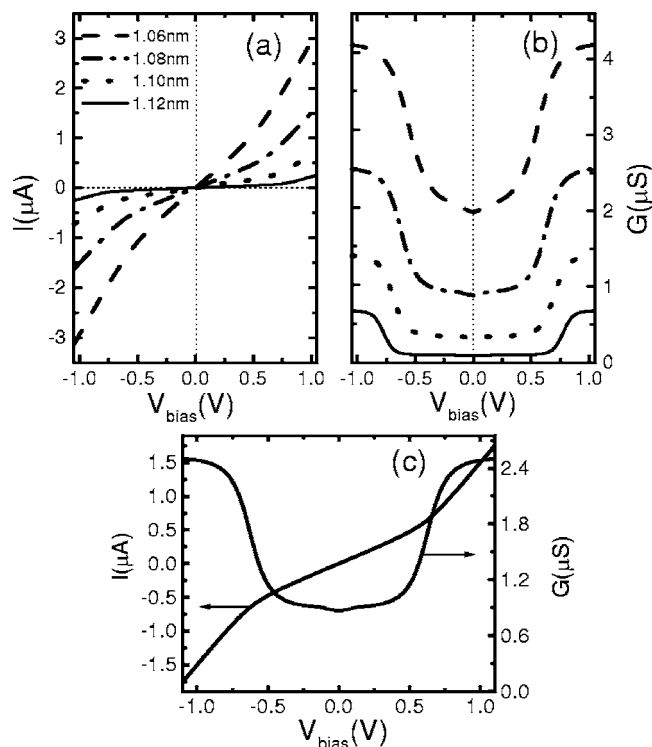


FIG. 5. Current (a) and conductance (b) curves of the molecular junction shown in Fig. 2(e). Distances of the two gold atoms nearest to the molecule are taken as $d=1.06$ nm (dashed line), 1.08 nm (dash-dotted line), 1.10 nm (dotted line), and 1.12 nm (solid line). (c) corresponds to the case of $d=1.08$ nm.

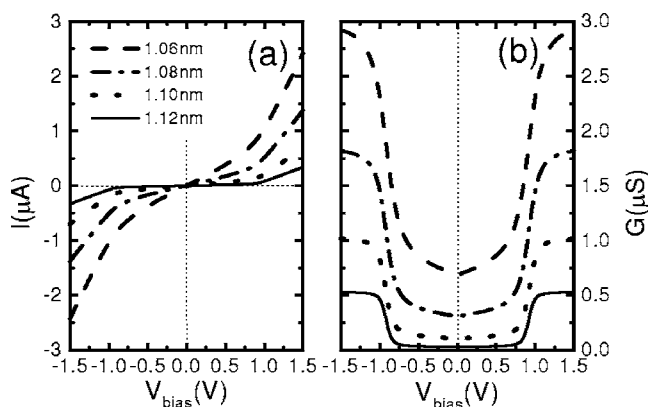


FIG. 6. Current (a) and conductance (b) curves of the molecular junction shown in Fig. 2(f). Distances of the two gold atoms nearest to the molecule are taken as $d=1.06$ nm (dashed line), 1.08 nm (dash-dotted line), 1.10 nm (dotted line), and 1.12 nm (solid line).

clusters. They still show similar features compared to those in Figs. 4 and 5. Nevertheless, the conductance plateau around zero bias shown in Fig. 6(b) is the lowest one among the three contact structures. It is noted that in the three contact configurations, the molecule is absorbed on top of one gold atom but with different surroundings. Therefore the couplings between the molecule and gold clusters are predicted to be different. Numerical analysis shows that the couplings between the nitrogen atom and gold cluster, Y_{1S} , are 3.37, 2.69, and 2.66 eV for cont1, cont2, and cont3, respectively, with the distance of 1.08 nm between the two gold clusters, which results in different values for the current and conductance in different contact structures. The similar

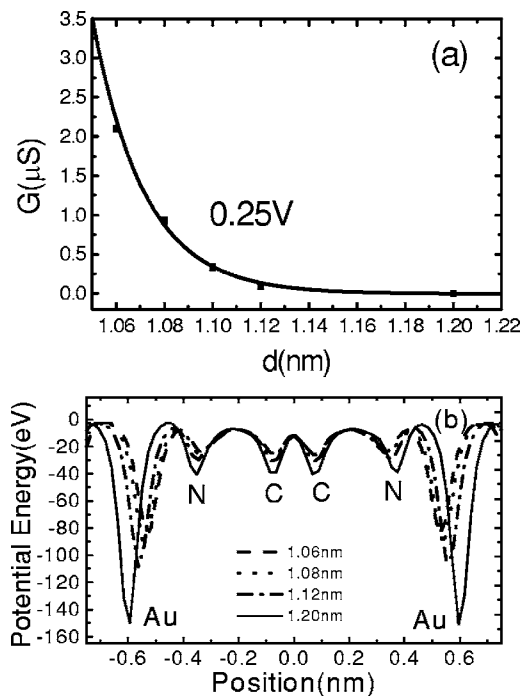


FIG. 7. The exponential relation between conductance and distance (a) at external bias 0.25 V and the potential distribution (b) for the molecular junction shown in Fig. 2(e).

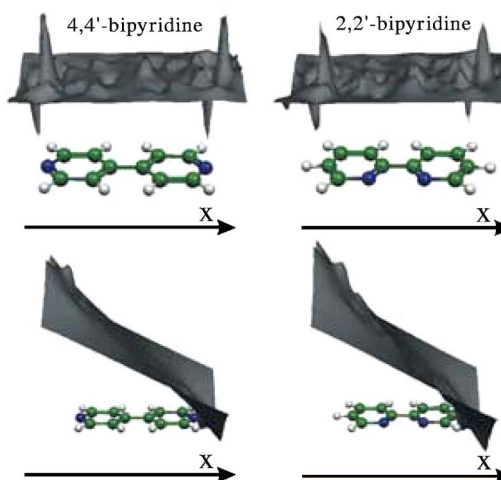


FIG. 8. (Color online) Spatial distribution of charge transfer and electrostatic potential drop for 4,4'-bipyridine and 2,2'-bipyridine molecular junctions at bias of 0.5 V.

current-voltage characteristics for the three different contact configurations indicate that the single gold atom interacting with the molecule directly plays the most important role.

According to the results mentioned above, one can see that the conductance of the device is very sensitive to the distance between two electrodes. For the 4,4'-bipyridine junction with gold atoms in a chain [see Fig. 2(e)], we have found that within the distances under investigation, the change of the conductance can be described by an exponential function of the distance, as clearly shown in Fig. 7(a) for the conductance at external bias of 0.25 V. Such a strong distance dependence can be understood by the fact that the coupling between molecule and metal in a physically adsorbed system can be exponentially dependent on the distance between them. To verify it, we have computed the coupling parameters between the atoms of the bare molecule and gold clusters. The numerical results show that the coupling parameters decrease with the increase of the distance between gold clusters. Reducing the distance can make the bare molecule coupled with gold clusters adequately and consequently lower the potential barriers between the molecule and gold clusters and reduce the depth of potential wells near the atomic nucleus for the electrons. Figure 7(b) shows the potential distribution for electrons along the molecular axis that passes through two nitrogen atoms. Each valley in the figure corresponds to the position of a nuclear. The calculated results show that the potential barrier between the molecule and gold atom decreases with shortening the distance. As expected, the shortening of the distance makes the electron tunneling through the junction easier, resulting in a larger conductance.

B. Nonlinear transport response

When the applied electronic fields are included, there exists charge response for the molecule.²⁶ The transport properties of the molecule are thus influenced by the applied bias voltage. As discussed by Xue and Ratner,²⁶ there exist two processes of charge transfer in molecular junctions when a

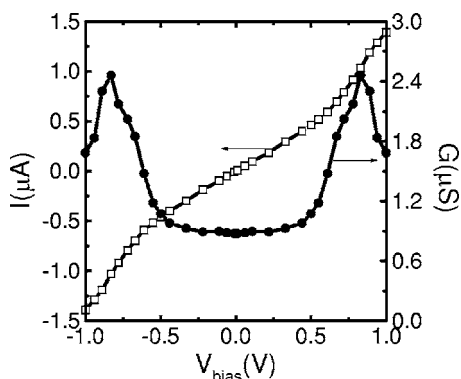


FIG. 9. The nonlinear transport properties of the molecular junction shown in Fig. 2(e) with the distance of two electrodes as $d = 1.08$ nm. The corresponding linear response is shown in Fig. 5(c).

bias is applied. One is the net charge injection into the molecule from electrodes, and the other is the charge redistribution inside the molecule. The charge redistributions for molecules at finite bias can be shown by plotting the spatial distributions of the transferred charge, where the difference in electron density at finite and zero biases is integrated along the z axis and the spatial distributions of the charge difference are obtained as a function of position in the xy plane. Figure 8 demonstrates the charge transferred process for 4,4'-bipyridine and 2,2'-bipyridine molecules at bias of 0.5 V. One can see that there are obvious variations of charge at ends of the molecules, while the variations inside the molecule are quite weak. Furthermore, electrons are accumulated on the injecting side from source because of the presence of potential barrier at the source-molecule contact, which inhibits the charge flow into the molecule. At the same time, the electrons are depleted on the extracting side of the potential barrier due to the flow of the π electrons inside the molecule in the direction of the negative x axis under the bias. This flow of the π electrons is impeded close to the nitrogen on the drain side, where accumulated charge appears, and the electrons are depleted at the molecule-drain contact. The charge redistribution results in two resistivity dipoles at the metal-molecule interfaces, which will lead to a nonlinear transport effect.²⁷ For the 2,2'-bipyridine molecule, the spatial distribution of transferred charge is similar to that for the 4,4'-bipyridine molecule. Nevertheless, the peak amount of the accumulated charge for 2,2'-bipyridine molecule is of $1.57 \times 10^{-3}/\text{a.u.}^2$, which is larger than that of $1.27 \times 10^{-3}/\text{a.u.}^2$ for the 4,4'-bipyridine molecule. This illustrates that the 2,2'-bipyridine molecule has more π electrons compared to the 4,4'-bipyridine molecule. As shown above, the amount of transferred charge is quite little under lower bias voltage, and it is then expected that the nonlinear transport effect is likely weak in the range of lower bias voltage. The electrostatic potential drop for both molecules

at bias voltage of 0.5 V is also shown in Fig. 8, which is evaluated by taking the difference of electrostatic potential between 0.5 V and zero biases. It is seen that the electrostatic potential drops rapidly in the region of molecule-electrode contacts and takes an almost linear variation inside the molecules.

The nonlinear charge transport properties of molecular junction shown in Fig. 2(e) are displayed in Fig. 9, where the geometrical structure is optimized and the electronic structure is obtained at each magnitude of the electric field. The current and conductance with including the nonlinear charge transport effect have almost the same values as the counterparts shown in Fig. 5(c). Otherwise, one can see from Fig. 9 that the feature of negative differential conductance appears at about bias voltage of 0.8 V.

IV. SUMMARY

In summary, we have studied the current-voltage characteristics of organic molecular 4,4'-bipyridine electronic devices by means of a generalized quantum chemical elastic scattering Green's function approach. The influence of different contact geometries between the molecule and gold electrodes on the electron transportation properties of the devices has been discussed in detail. It is found that the energetically favorable bonding site for nitrogen atoms is on top of a gold atom. A similar distance dependence has been observed for contacts with planar, chain, or pyramid configurations, indicating that the major contribution comes from the gold atom that is bonded to the molecule. This can be well understood by the fact that the conductance is exponentially dependent on the distance between the molecule and electrodes. Such a distance dependence is a result of the strong distance dependence of the couplings between them. In general, one can find that the shorter the distance, the stronger the coupling, the lower the potential barrier, and consequently the larger the conductance will be. Good agreement between theory and experiment can be achieved when the contacts are of chain configuration and separated by a distance of 1.08 nm. When the electric field is considered, two kinds of charge transfer process are demonstrated and the charge redistribution leads to the presence of resistivity dipoles at the molecule-metal interfaces. When the bias voltage is in the lower region, the charge transport properties of 4,4'-bipyridine molecular junctions are a little influenced except for the appearance of the negative differential conductance.

ACKNOWLEDGMENTS

The authors thank the support of the National Nature Science Foundation of China (Grant No. 10274044), Swedish Research Council, and Swedish International Development Cooperation Agency (Sida).

*Electronic address: ckwang@sdnu.edu.cn

- ¹M. A. Reed, C. Zhou, C. J. Muller, T. P. Burgin, and J. M. Tour, *Science* **278**, 252 (1997).
- ²S. Frank, P. Poncharal, Z. L. Wang, and W. A. de Heer, *Science* **280**, 1744 (1998).
- ³J. Chen, M. A. Reed, A. M. Rawlett, and J. M. Tour, *Science* **286**, 1550 (1999).
- ⁴A. N. Pasupathy, R. C. Bialczak, J. Martinek, J. E. Grose, L. A. K. Donev, P. L. McEuen, and D. C. Ralph, *Science* **306**, 86 (2004).
- ⁵Sz. Csonka, A. Halbritter, G. Mihály, O. I. Shklyarevskii, S. Speller, and H. van Kempen, *Phys. Rev. Lett.* **93**, 016802 (2004).
- ⁶S. Yasutomi, T. Morita, Y. Imanishi, and S. Kimura, *Science* **304**, 1944 (2004).
- ⁷G. V. Nazin, X. H. Qiu, and W. Ho, *Science* **302**, 77 (2003).
- ⁸B.-Q. Xu and N. J. Tao, *Science* **301**, 1221 (2003).
- ⁹J. Jiang, W. Lu, and Y. Luo, *Chem. Phys. Lett.* **400**, 336 (2004).
- ¹⁰M. D. Ventra, N. D. Lang, and S. T. Pantelides, *Chem. Phys.* **281**, 189 (2002).
- ¹¹E. G. Emberly and G. Kirczenow, *Chem. Phys.* **281**, 311 (2002).
- ¹²P. S. Damle, A. W. Ghosh, and S. Datta, *Phys. Rev. B* **64**, 201403 (2001).
- ¹³J. Taylow, M. Brandbyge, and K. Stokbro, *Phys. Rev. B* **68**, 121101 (2003).
- ¹⁴C.-K. Wang, Y. Fu, and Y. Luo, *Phys. Chem. Chem. Phys.* **3**, 5017 (2001).
- ¹⁵Y. Luo, C.-K. Wang, and Y. Fu, *J. Chem. Phys.* **117**, 10283 (2002).
- ¹⁶C.-K. Wang and Y. Luo, *J. Chem. Phys.* **119**, 4923 (2003).
- ¹⁷Y. Luo, C.-K. Wang, and Y. Fu, *Chem. Phys. Lett.* **369**, 299 (2003).
- ¹⁸Jun Jiang and Yi Luo, computer code QCME-V1.0 (quantum chemistry for molecular electronics), 2004, Stockholm (thanks to Chuan-Kui Wang and Ying Fu).
- ¹⁹J. Tersoff and D. R. Hamann, *Phys. Rev. B* **31**, 805 (1985).
- ²⁰V. Mujica, M. Kemp, and M. A. Ratner, *J. Chem. Phys.* **101**, 6849 (1994).
- ²¹W. Tian, S. Datta, S. Hong, R. Reifenberger, J. I. Henderson, and C. P. Kubiak, *J. Chem. Phys.* **109**, 2874 (1998).
- ²²D. M. Newns, *Phys. Rev.* **178**, 1123 (1969).
- ²³M. J. Frisch *et al.*, computer code GAUSSIAN 98, Gaussian Inc, Pittsburgh, PA, 1998.
- ²⁴J. C. Cuevas, A. Levy Yeyati, and A. Martín-Rodero, *Phys. Rev. Lett.* **80**, 1066 (1998).
- ²⁵J. Heurich, J. C. Cuevas, W. Wenzel, and G. Schön, *Phys. Rev. Lett.* **88**, 256803 (2002).
- ²⁶Y. Xue and M. A. Ratner, *Phys. Rev. B* **68**, 115406 (2003).
- ²⁷R. Landauer, *IBM J. Res. Dev.* **1**, 223 (1957); **32**, 306 (1988).